ELSEVIER

Polymer 44 (2003) 1057–1065

polymer

www.elsevier.com/locate/polymer

Ionic conductivity of chitosan membranes

Ying Wan, Katherine A.M. Creber*, Brant Peppley, V. Tam Bui

Department of Chemistry and Chemical Engineering, Royal Military College of Canada, P.O. Box 17000, Station Forces, Kingston, Ont., Canada, K7K 7B4

Received 14 May 2002; received in revised form 18 November 2002; accepted 20 November 2002

Abstract

Chitosan membranes with various degrees of deacetylation and different molecular weights (MW) were prepared by film casting with aqueous solutions of chitosan and acetic acid. Ultraviolet (UV) spectrometry and infrared (IR) spectrometry were used to determine the degree of deacetylation (DDA) of chitosan. The viscosity–average MW of chitosan was measured in an aqueous solvent system of 0.25 M CH_3COOH/0.25 M CH_3COONa. The intrinsic ionic conductivities of the hydrated chitosan membranes were investigated using impedance spectroscopy. It was found that the intrinsic ionic conductivity was as high as 10^{-4} S cm^{-1} after hydration for 1 h. The tensile strength and breaking elongation of the membranes were evaluated according to standard ASTM methods. The crystallinity and swelling ratio of the membranes were examined. A tentative mechanism for the ionic conductivity of chitosan membranes is also suggested.

Keywords: Chitosan membrane; Hydration; Ionic conductivity

1. Introduction

Chitin, a (1–4)-linked 2-acetamido-2-deoxy-β-D-glucan, is a natural polysaccharide that occurs mainly in insects, marine invertebrates, fungi, and yeasts. It is also one of the most abundant natural polymers next to cellulose. Chitosan is the N-deacetylated derivative of chitin. It is generally accepted that this biopolymer is referred as 'chitosan' if chitin is N-deacetylated to such a degree that it becomes soluble in dilute aqueous acidic systems. Fig. 1 illustrates the molecular structures of segments of chitin and chitosan [1].

Chitosan has recently aroused a great deal of interest in view of its industrial and biomedical applications [2]. Chitosan also has a high potential for development into sophisticated functional polymers quite different from those of synthetic polymers since it has both free amino groups and hydroxyl groups on its backbone, which are easily modified by many organic reactions (tosylation [3], alkylation [4], carbocylation [5], sulfonation [6], Schiff base [7], quaternary salt [8] and so on). As a copolymer, chitosan is readily converted to fibers, films, coatings, and beads as well as powders and solutions, further enhancing its usefulness. Applications are numerous, including such areas as pharmaceutical and biomedical engineering, paper production, textile finishes, photographic products, cements, heavy metal chelation, waste water treatment, and fiber and film formation [9,10].

Chitosan can also act as a cationic polyelectrolyte because of its free amino groups [11]. With respect to its ionic properties, the chitosan membrane has been used for chloride-ions-conducting [12]. In a similar way, when a chitosan membrane is swollen in water the amino groups may be protonated and leaving the hydroxide ions free in water, which may contribute to the ionic conduction in the membrane. However, in this case, since there is not any electrolyte being added to the membrane before it was made the ionic conduction that membrane may show will be an intrinsic ionic conduction.

In this study, many chitosan membranes with various degrees of deacetylation and different molecular weights (MW) were prepared by the film-casting method from aqueous solutions of chitosan and acetic acid. Although physical properties such as crystallinity, swelling ratio, tensile strength and elongation as a function of the degree of deacetylation (DDA) and MW of chitosan have been previously investigated, it was necessary to do a comprehensive report as a baseline for our study. This paper reports the first results of our study of the intrinsic ionic

* Corresponding author. Tel.: +1-613-541-6000x6049; fax: +1-613-542-9489.

E-mail address: creber@rmc.ca (K.A.M. Creber).

0032-3861/03/$ - see front matter © 2002 Published by Elsevier Science Ltd.
PII: S0032-3861(02)00881-9

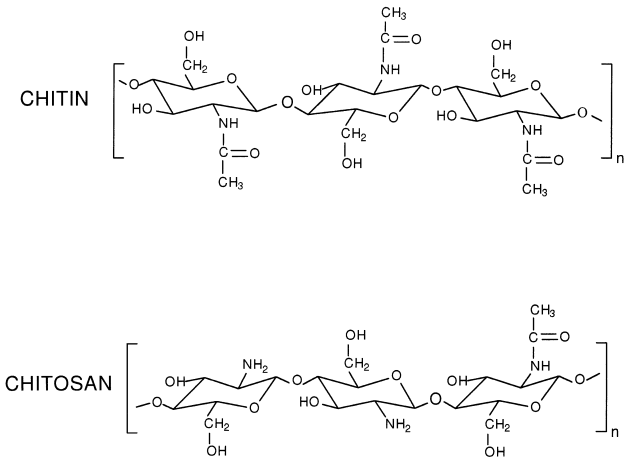

Fig. 1. Segments of chitin and chitosan.

conductivity of hydrated chitosan membranes and correlates this with the DDA, MW and physical properties of the membranes.

2. Experimental

2.1. Materials

Three kinds of chitosans were obtained as powder or flakes from Sigma-Aldrich Canada Ltd. The claimed viscosity values of solutions of 1% these chitosans (by weight) in 1% (by volume) aqueous acetic acid were provided as 800–2000, 200–800 and 20–200 cps, and their molecular weights (MW) were claimed as high MW, medium MW and low MW, respectively. These three kinds of original chitosans were designated as Ch-I (high MW), Ch-II (medium MW) and Ch-III (low MW), respectively, and the other deacetylated chitosan samples were made from them. The following chemicals were all obtained and used as reagent grade from either Sigma–Aldrich Canada Ltd. or Caledon Laboratories Ltd.: acetic acid, sodium acetate, ammonium hydroxide (38%), sodium hydroxide pellets, acetic anhydride, methanol, *N*-acetyl-D-glucosamine (NAG, 99%, FW 221.21), potassium bromide. The deionized water (resistivity $> 1.8 \times 10^8\ \Omega$ cm) was used for all samples.

2.2. Deacetylation and reacetylation

To increase the amine group content of chitosan, it was further deacetylated according to a reported method. It is somewhat difficult to completely deacetylate chitosan. One of methods to obtain a higher deacetylated chitosan (for example, DDA > 90%) is repeating alkaline treatment [13]. Ch-I, Ch-II and Ch-III, therefore, were treated in 50% NaOH solution (by weight) for 1 h in a reactor at 100 °C under air. After washing repeatedly and drying, the corresponding products were designated as Ch-H, Ch-M and Ch-L. Then Ch-H, Ch-M and Ch-L were further deacetylated with the same conditions, respectively, removing samples every hour to yield three sets of chitosan samples with different degrees of deacetylation in the range from about 80 to 96%.

To obtain a series of chitosan samples with similar MW but varied degrees of deacetylation, a reported method was followed [14]. Five samples (4 g) of Ch-H-3 (refer to notes under Table 1) were each dissolved in 200 ml of 1% aqueous acetic acid. 200 ml of methanol was added to each solution and stirred for a further 20 min. The final addition to each solution included 100 ml of methanol containing acetic anhydride, ranging in amount from 1.98×10^{-3} mol for sample Ch-H-A to 1.37×10^{-2} mol for sample Ch-H-E. The solutions were then stirred for a further 20 h at room temperature. At the end of the reaction, methanolic ammonia was added to each solution in order to precipitate the chitosan. The precipitants were washed intensively with deionized water until neutrality. The solids were finally dried in a convection oven at 50 °C for 3 days and then in a vacuum oven at 50 °C for 12 h.

2.3. Degree of deacetylation

The DDA was determined by first derivative UV (ultraviolet) spectroscopy. UV spectra were recorded on a CARY 5E UV–Vis-NIR spectrometer, following a reported method [15]. To begin the procedure, a calibration curve was obtained with slope of absorbance at nm versus concentration of *N*-acetyl-D-glucosamine (NAG) in units of mg/ml. All chitosan samples analyzed using UV absorption spectroscopy (0.5000 ± 0.0026 g) were dissolved in 100 ml of 1% (v/v) aqueous acetic acid. Using a Pasteur pipette, an aliquot (2.0 ± 0.1 g) of the chitosan solution was further diluted with another 100 ml of 1% (v/v) aqueous acetic acid. The resulting absorbance values were plotted on the calibration curve, and corresponding concentrations of NAG in mg/ml were read. The DDA values were calculated by the reported method [16].

The water content of chitosan samples was determined using a Texas Instruments 2050 TGA Thermogravimetric Analyzer. The sample was heated from 25 to 300 °C at 10 °C/min under nitrogen. The loss in weight of the chitosan sample of 180 °C was taken to be the result of water evaporation. The error in water content value of chitosan was the largest contributing factor to the error in the DDA calculation.

In order to compare the results obtained with different methods, the DDA was also determined by infrared (IR) spectroscopy [17]. The chitosan powders were first dried in a vacuum oven at 50 °C until constant weight and a well-mixed mixture of chitosan and KBr at a ratio of 2:100 was made into a disc. FTIR spectra were recorded on a Nicolet 510P spectrometer and the DDA was calculated by Eq. (1):

$$\mathrm{DDA} = 100 - (A_{1655}/A_{3450})115 \quad (1)$$

Table 1
Deacetylated and reacetylated chitosan sample information

Sample code	% DDA (±3.8%) UV	% DDA (±5.5%) FTIR	% Water + impurities (±1.7%)	M_v (±5.4%)	Deacetylation/reacetylation conditions
Ch-H-1[a]	84.4	82.6	4.1	1.0×10^6	
Ch-H-1	90.6	88.4	5.2	8.9×10^5	Ch-H, 1 h, 50% $NaOH_{(AQ)}$, 100 °C, air
Ch-H-2	93.8	94.6	3.8	8.1×10^5	Ch-H, 2 h
Ch-H-3	95.4	93.8	3.3	7.8×10^5	Ch-H, 3 h
Ch-H-4	95.3	95.1	4.7	7.1×10^5	Ch-H, 4 h
Ch-H-5	95.7	94.3	4.1	6.5×10^5	Ch-H, 5 h
Ch-H-6	95.1	93.4	3.4	5.9×10^5	Ch-H, 6 h
Ch-M[b]	83.3	81.2	4.5	7.2×10^5	
Ch-M-1	91.4	87.5	3.3	6.1×10^5	Ch-M, 1 h, 50% $NaOH_{(AQ)}$, 100 °C, air
Ch-M-2	93.1	90.1	4.6	5.7×10^5	Ch-M, 2 h
Ch-M-3	94.5	92.7	4.3	5.4×10^5	Ch-M, 3 h
Ch-M-4	95.6	94.2	3.2	4.9×10^5	Ch-M, 4 h
Ch-M-5	95.1	96.3	4.2	4.8×10^5	Ch-M, 5 h
Ch-M-6	95.4	93.1	4.9	4.9×10^5	Ch-M, 6 h
Ch-L[c]	82.7	84.3	4.7	3.7×10^5	
Ch-L-1	90.5	89.7	3.7	3.2×10^5	Ch-L, 1 h, 50% $NaOH_{(AQ)}$, 100 °C, air
Ch-L-2	92.3	87.6	3.6	3.1×10^5	Ch-L, 2 h
Ch-L-4	94.2	93.5	44	2.9×10^5	Ch-L, 4 h
Reacetylated samples[d]					
Ch-H-A	91.7	92.1	4.1	7.5×10^5	Ch-H-3 + $(CH_3CO)_2O$ (0.2019 g)
Ch-H-B	88.3	85.7	3.8	7.5×10^5	Ch-H-3 + $(CH_3CO)_2O$ (0.2475 g)
Ch-H-C	84.2	80.8	3.2	7.4×10^5	Ch-H-3 + $(CH_3CO)_2O$ (0.2894 g)
Ch-H-D	78.4	77.3	3.1	7.4×10^5	Ch-H-3 + $(CH_3CO)_2O$ (0.5691 g)
Ch-H-E	70.7	66.1	4.9	7.3×10^5	Ch-H-3 + $(CH_3CO)_2O$ (1.4003 g)

[a] Ch-H was made by deacetylating Ch-I for 1 h in 50 wt% NaOH solution at 100 °C under air. H and *i* in Ch-H-*i* ($i = 1,\ldots,6$) refer to high MW for chitosan, and hours for further deacetylation, respectively.
[b] Ch-M was made by deacetylating Ch-II for 1 h in 50 wt% NaOH solution at 100 °C under air. M and *j* in Ch-M-*j* ($j = 1, \ldots, 6$) refer to medium MW for chitosan, and hours for further deacetylation, respectively.
[c] Ch-L was made by deacetylating Ch-III for 1 h in 50 wt% NaOH solution at 100 °C under air. L and *k* in Ch-L-*k* ($k = 1, 2, 4$) refer to low MW for chitosan, and hours for further deacetylation, respectively.
[d] This series of chitosan samples was obtained by reacetylating Ch-H-3 with various amount of acetic anhydride under the same conditions.

where A_{1655} is the peak area of the amide I band at 1655 cm^{-1}, and A_{3450} is the peak area of the OH band at 3450 cm^{-1}. The results quoted are the average values from three specimens of each sample.

2.4. Viscometry measurements

The viscosities of chitosan samples were measured in a solvent system of 0.25 M CH_3COOH/0.25 M CH_3COONa using an Ubbelohde capillary viscometer (model CANNON 75 F107) which yielded an average flow time of 110.47 ± 0.1 s in a viscometer bath at 24.95 ± 0.05 °C for this solvent system. The overall error in the intrinsic viscosity, resulting mainly from the flow time and concentration uncertainties, and the temperature fluctuation, was estimated as being ±0.74 dl/g, which led to a maximum error of ±5.4% in the value of viscosity–average MW.

2.5. Preparation of membrane

Chitosan solutions were prepared by dissolving about 1–2 g of chitosan in 100 ml of 1% (v/v) aqueous acetic acid solution. The solution was filtered in order to remove undissolved chitosan and debris, and then was cast onto a Petri dish. The transparent membranes were obtained after drying in air for 48 h. All dried membranes were mounted on a stainless steel holding device and immersed in 2% NaOH aqueous solution for a given time to ensure the complete removal of residual acid from the membranes. These membranes were washed thoroughly in deionized water until a neutral pH, dried in air for 48 h and then in vacuum at 50–60 °C for 24 h. All membranes had a thickness of about 90–130 μm.

2.6. Crystallinity of membranes

The X-ray diffraction (XRD) patterns of the membranes with around 100 μm thickness were recorded with a SCINTAG X1 X-ray diffractrometer and used a Cu Kα target at 45 kV and 40 mA. The diffraction angle was varied from 45 to 2°. The crystallinities (X_c) of the membranes were estimated by Eq. (2) [18]:

$$X_c = [F_c/(F_c + F_a)]100\% \quad (2)$$

where F_c and F_a are the areas of crystal and non-crystalline regions, respectively.

2.7. Swelling index measurements

The dried membrane (mass = W_d) was immersed in an excess amount of deionized water at ambient temperature until swelling equilibrium was attained. The mass of wet sample (W_w) was measured after removing the surface water with blotting paper. The Swelling index (SI) was then calculated on the basis of the masses of wet membrane and dry membrane:

$$SI = [(W_w - W_d/W_d)]100\% \quad (3)$$

2.8. Ionic conductivity measurements

The ionic conductivity measurements were made by following a reported method [19]. A Hewlett-Packard Impedance/Gain-phase Analyzer (model 4194A) was used for impedance spectroscopy analysis of the membranes. Complex impedance measurements were carried out in AC mode, in the frequency range $0.1-10^4$ kHz, and 1 V amplitude of the applied AC signal. The dry membranes were sandwiched between two brass blocking electrodes in the measurement cell. For impedance analysis in the swollen state, the membranes were immersed in deionized water at room temperature for the required time. Prior to any measurement, the surface water was properly removed, and then the swollen membrane was quickly placed between electrodes in the measurement cell. The water content of the membrane was assumed to remain constant during the short period of time required for the measurement.

2.9. Mechanical testing

The mechanical properties of membranes were mainly evaluated by the tensile test. This was performed using a tensile testing machine (INSTRON 4206, USA) according to the standard method (ASTM D882). The testing specimens were cut into strips with 70 mm length and 25 mm width with an accuracy of ± 5 μm. The relative humidity, gauge length and the crosshead speed were 50%, 30 mm and 5 mm/min, respectively. All specimens were drawn at ambient temperature and ultimate tensile strength and breaking elongation were instantaneously recorded using a computer. At least five specimens were measured for each sample.

3. Results and discussion

3.1. Degree of deacetylation and viscosity average molecular weight

Since the higher content of amino groups in chitosan membranes may contribute a higher ionic conductivity, the chitosans have been deacetylated before they are used to prepare membranes. In order to find out the effect of chitosan with similar MW but varied DDA on the properties of membranes, a chitosan sample with higher MW and a deacetylation ca. 95% was reacetylated again. Table 1 summarizes all relevant information concerning the deacetylated and reacetylated chitosan samples obtained from the original samples, Ch-I–Ch-III. Usually, with increasing reaction times and temperature, the DDA will increase, but chitin will be degraded. As can be seen in Table 1, some chitosan samples obtained have shown as high as 95% DDA and have not been substantially degraded compared to the original chitosan samples. By reacetylating Ch-H-3, five samples with different DDA values have been obtained. The DDA values of these reacetylated samples have been changed pronouncedly while their MW have been maintained.

Viscometry is the most common method for determining the MW of polymers by using Mark–Houwink–Sakurada equation. The use of viscometry in the case of chitosan, however, is not always straightforward because of its complex hydrodynamic behaviour, which greatly depends upon its DDA and the solvent system used, as well as temperature. Several authors have reported different coefficient and exponent values in Mark–Houwink–Sakurada equation for chitosans of varying DDA, in various solvent systems [20]. The 0.25 M CH_3COOH/0.25 M CH_3COONa solvent system has been chosen here because the viscosity–average MW of chitosan obtained using this solvent system is almost independent of its DDA in a range above 60%. With this solvent system, the viscosity–average MW of chitosan will be determined by the following equation [21]:

$$[\eta] = 1.40 \times 10^{-4} M_v^{0.83} \quad (4)$$

There are numerous available methods for measuring the DDA of chitosan. The most common technologies are [22]: elemental analysis, IR spectroscopy, NMR spectroscopy and UV spectroscopy, though the stated methods are not completely reliable over the full range of deacetylation values from 0 to 100%. First derivative UV spectroscopy and IR spectroscopy have been employed in this study because they are relatively quick and accurate. By comparing the DDA values obtained from UV spectroscopy with those from FTIR spectroscopy, shown in Table 1, it is observed that there is a relatively large uncertainty when the FTIR spectroscopy method is employed. This is likely related to the water content in the chitosan samples by which the absorbance of OH band at 3450 cm^{-1} is somewhat affected and in turn the calculation of DDA values. Consequently, the DDA results obtained from UV spectroscopy will be used in the following sections.

3.2. Effect of DDA of chitosan on the properties of membranes

The variance of properties of membranes having similar MW but varied DDA in dry state is represented in Figs. 2

and 3. It is noted that the DDA of chitosan has obviously affected crystallinity, mechanical and swelling properties of membranes. The X-ray patterns of these membranes are shown in Fig. 4. The diffractogram of the membranes consists of three major crystalline peaks at 2θ, 10.5, 15.4 and 20.1°, which are in agreement with Samuels' report [23]. The diffraction patterns of membranes remain almost the same for the four membranes made from different DDA chitosans. This may suggest that the crystal structure in these membranes was maintained basically the same even though their DDA varied. However, from Fig. 2, the crystallinity of the membrane increases gradually with increasing DDA ranging from 70 to 92%. This may be attributed to the fact that chains of chitosan with higher DDA are more flexible [24]. Flexible chains of chitosan will facilitate the hydrogen-bonding formation and in turn crystallinity formation in the membrane. Furthermore, higher DDA chitosan contains more glucoseamine groups that also facilitate hydrogen-bonding formation. On the contrary, lower DDA chitosan has more acetyl groups that hinder the hydrogen-bonding formation due to their rigidity and steric effect. Therefore, the membranes prepared from high DDA chitosan contain a larger crystalline region.

Fig. 3 represents the tensile strength of the membranes, which increases with the increase in DDA of chitosans used, but the alteration of breaking elongation expresses a tendency contrary to that of tensile strength. Normally, the larger crystalline regions in membranes will enhance the mechanical strength of the membrane [25], however, they may increase the fragility of membrane resulting in a lower breaking elongation. Thus, the membrane made from high DDA chitosan, which contains more crystallinity and has a larger tensile strength, shows a lower breaking elongation. A similar result that the breaking elongation of the membrane decreased with increasing DDA and decreasing MW of the chitosan has also been observed by other authors although the reported trend was not significant [26].

The swelling property of the membrane will affect the

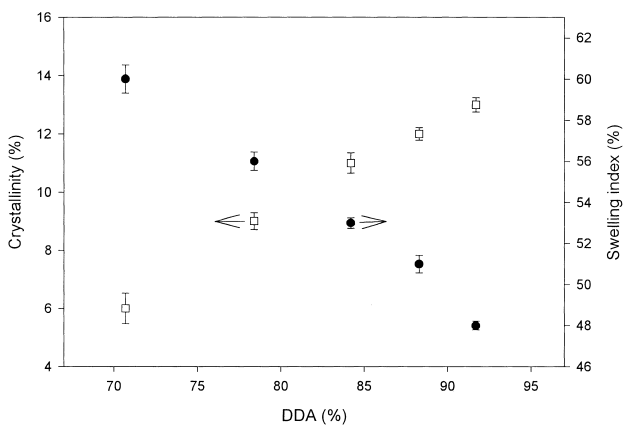

Fig. 2. The variance of crystallinity and SI of chitosan membranes with DDA (the viscosity–average MW of chitosan is ca. 7.4×10^5).

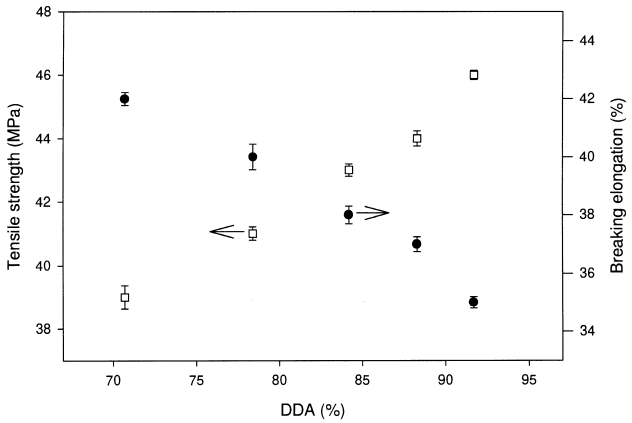

Fig. 3. The dependence of tensile strength and breaking elongation of chitosan membranes on the DDA.

ion permeability through the membrane. A relatively high SI of the membrane will allow ions to go through the membrane more easily in the swollen state. The results given in Fig. 2 indicate that the SI of the membrane prepared from lower DDA chitosan is larger than that of those membranes from higher DDA chitosan. It is known that the hydrophilic groups, i.e. hydroxyl groups and amine groups on the backbone of chitosan, cause swelling of chitosan membranes. On the other hand, the increase of the DDA of chitosan will lead to a higher amine group content on the backbone of chitosan, which seems to enhance the hydrophilicity of the membranes and in turn an increase in the SI. In fact, the SI of the membranes drops off as the higher DDA chitosans are employed. This SI behavior may suggest that interaction from the intramolecular hydrogen bonds between hydroxyl groups and amine groups is much stronger than that from intermolecular hydrogen bonds between these polar groups and water. As a result, the high crystallinity of the membrane prepared from high DDA chitosan prevents water from entering the grown crystalline

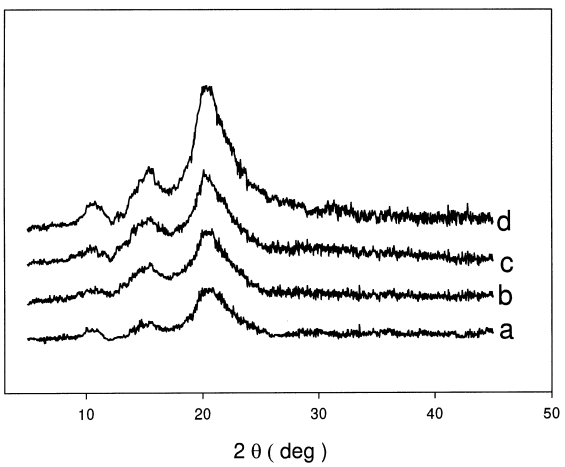

Fig. 4. XRD patterns of chitosan membranes with various DDA and similar MW, (a): DDA = 70.0%, MW = 739.4×10^3; (b): DDA = 78.4%, MW = 748.6×10^3; (c): DDA = 84.2%, MW = 747.6×10^3; (d): DDA = 91.7%, MW = 753.3×10^3.

portion and renders resistance to water, and finally hinders the swelling of the membrane.

3.3. Effect of molecular weight of chitosan on the properties of the membrane

Effects of MW of chitosan on the crystallinity, mechanical and swelling properties of membranes are illustrated in Figs. 5 and 6. Three X-ray patterns for the membranes with similar DDA but various MW are shown in Fig. 7. Except for the strength of diffractive peaks, it is noted that the diffraction patterns of membranes are kept almost the same. From Figs. 5 and 7, it is observed that the membrane prepared from higher-molecular-weight chitosan produces a less crystalline membrane. This is in agreement with the reported result [27]. In general, the higher the MW of chitosan used, the larger the tensile strength of the membrane [28]; this is well illustrated by Fig. 6. In addition, the chitosan membrane with high crystallinity seems to have a larger tensile strength when the only factor, crystallinity of membrane, has been considered. The results obtained in Figs. 5 and 6, however, show that the MW of chitosan is the dominant effect on the tensile strength of the membrane. For the same DDA, the tensile strength of a membrane with a high MW and a low crystallinity is stronger than that with a low MW and a high crystallinity. The breaking elongation of the membranes tends to decrease gradually with decreased MW of chitosan and the SI of membranes also shows a similar tendency. The behavior of breaking elongation is probably due to longer chain length and more entangled chains in high-molecular-weight chitosans compared to the low-molecular-weight chitosans, which allows the chitosan molecules to extend much further under the stress, and in turn larger elongation of the membranes. As for the alternation of SI, the conclusion can be drawn that the higher crystallinity in the membrane prepared from low-molecular-weight chitosan hinders the swelling of the membrane.

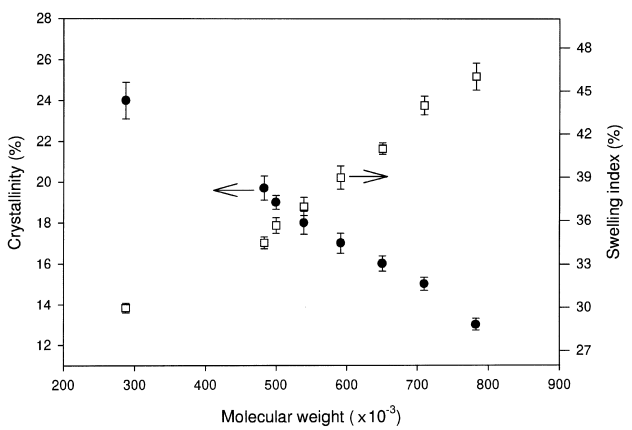

Fig. 5. The variance of crystallinity and SI of chitosan membranes with MW (the DDA of chitosan is ca. 95%).

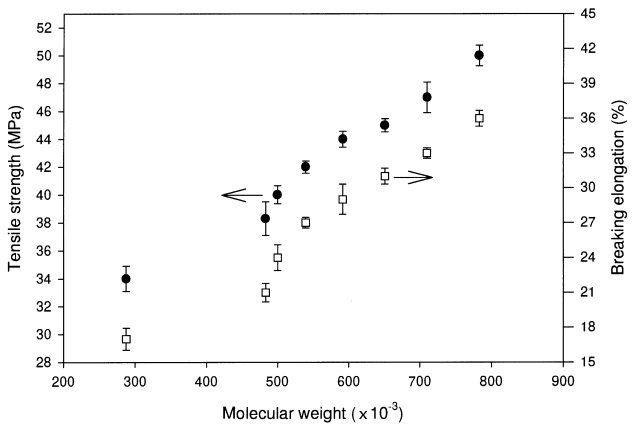

Fig. 6. The dependence of tensile strength and breaking elongation of chitosan membranes on the MW (the DDA of chitosan is ca. 95%).

3.4. Ionic conductivity of membrane

3.4.1. Interpretation of impedance spectra

Ionic conductivity of the chitosan membranes was determined using the complex impedance method. All impedance measurements were done before and after hydration of the membranes. Membranes in dry form exhibit ionic conductivities between 10^{-9} and 10^{-10} S cm^{-1} and the entire conduction process occurs through the water incorporated in the membranes. Typical plots of imaginary impedance ($-Z''$) versus real impedance (Z') for the membranes with varied DDA and the membranes with varied MW after hydration for 1 h at room temperature are shown in Figs. 8 and 9, respectively. In addition, the complex impedance plot of Ch-H-3 with varied hydration time are illustrated in Fig. 10. These spectra comprise two well-defined regions in the complex-plane, a typical partial arc in the high frequency zone that is related to the conduction process in the bulk of the membrane, and a linear region in the low frequency zone, being related to the existence of concentration gradients that

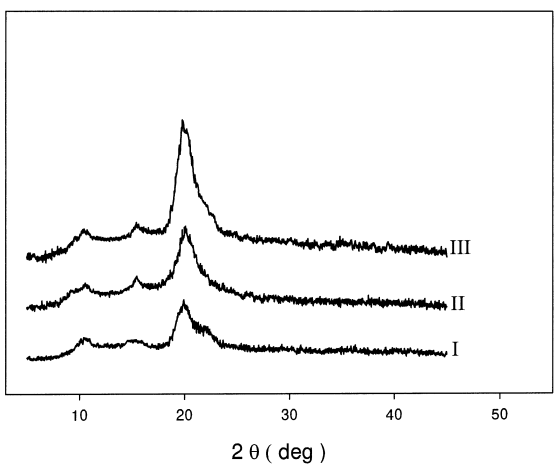

Fig. 7. XRD patterns of chitosan membranes with various MW and similar DDA (I): DDA = 95.4%, MW = 787.7 × 10^3; (II): DDA = 94.5%, MW = 539.5 × 10^3; (III): DDA = 94.2%, MW = 287.5 × 10^3.

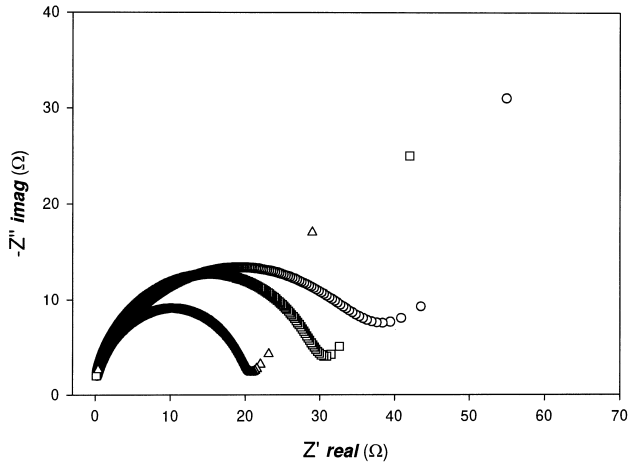

Fig. 8. Impedance spectra obtained for membranes with varied DDA and similar MW after hydration for 1 h at room temperature. AC mode; 1 V amplitude of applied signal; frequency range: $0.1-10^4$ kHz; (○) Ch-H-A; (□) Ch-H-B; (△) Ch-H-D.

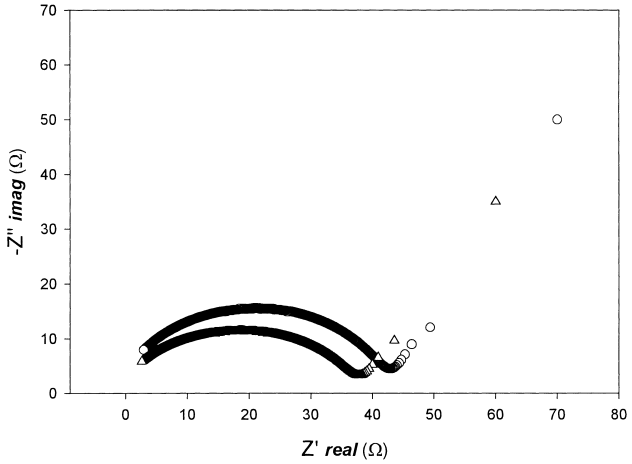

Fig. 10. Impedance spectra obtained for membranes Ch-H-3 after hydration for 1 and 24 h at room temperature. Other testing conditions are the same as Fig. 8. (○) 1 h (Ch-H-3); (△) 24 h (Ch-H-3).

give rise to diffusion processes in the bulk electrolyte [29]. Since the complex impedance will be dominated by the ionic conductance when the phase angle is close to zero, normally, the bulk resistance is directly obtained from the intercept of complex impedance plot with real axis (Z' axis). From Figs. 8 and 9, some complex impedance curves have not touched the real axis though they are near to the real axis. For these cases, the complex impedance plot is extrapolated to its intersection with the real axis and the conductivity of membrane is calculated with Osman's method [30].

3.4.2. Mechanism of hydroxyl conductivity

Conductivities of membrane before and after hydration are shown in Figs. 11 and 12, respectively. From Fig. 11, the DDA of chitosan affects slightly the ionic conductivity of membrane, that is, the conductivity of the membrane increases slightly with decreasing DDA of chitosan. It is also observed from Fig. 12 that the membranes prepared with high MW chitosan show a relatively high conductivity. As pointed out above, the ionic conductance will occur only after the membrane is hydrated. This may be explained based on the following tentative mechanism which is shown in Fig. 13. When water is incorporated into chitosan membranes, the free amino groups in the chitosan backbone, which are weak alkaline groups, are partially protonated ($NH_2 + H_2O \leftrightarrow NH_3^+ + OH^-$) also forming some hydroxide ions. Since the NH_3^+ groups are bonded on the backbone and OH^- ions are free to move and give an ionic current under the action of AC signal. According to this tentative mechanism, it seems that the membrane with higher DDA, which contains more NH_2 groups compared to a lower DDA chitosan membrane, should give a higher ionic conductivity. However, by using high DDA chitosan or low MW chitosan, substantial crystalline regions will be obtained such that water is prevented from entering the crystalline portion and a large resistance is rendered to water incorporation. This finally decreases the concentration of OH^- groups in the

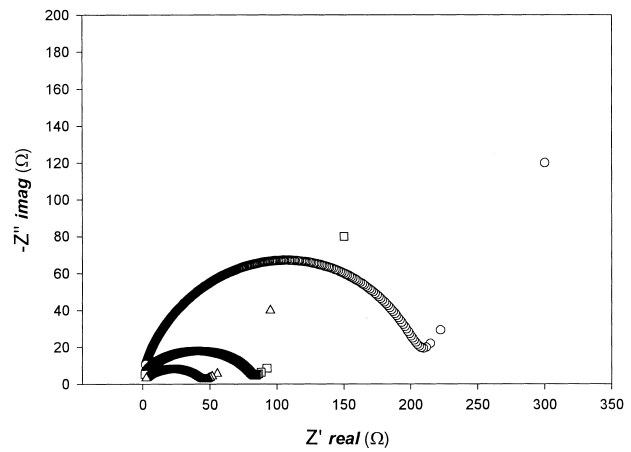

Fig. 9. Impedance spectra obtained for membranes with varied MW and similar DDA after hydration for 1 h at room temperature. Testing conditions are the same as Fig. 8. (○) Ch-L-4; (□) Ch-M-4; (△) Ch-H-4.

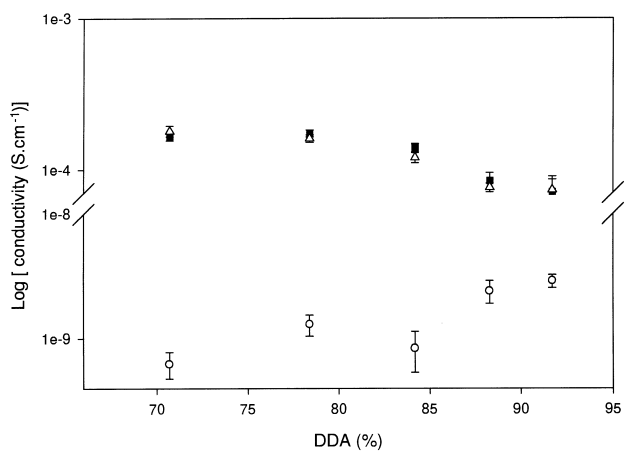

Fig. 11. Ionic conductivity of membranes with varied DDA before and after hydration (the viscosity–average MW of chitosan is ca. 7.4×10^5); (○) before hydration; (■) after hydration for 1 h; (△) after hydration for 24 h.

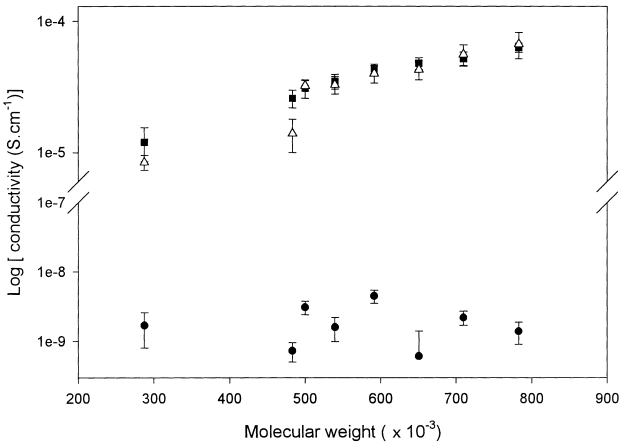

Fig. 12. Ionic conductivity of membranes with varied MW before and after hydration (the DDA of chitosan is ca. 95%); (●) before hydration; (■) after hydration for 1 h; (△) after hydration for 24 h.

swollen membrane and in turn the ionic conductivity of the membrane. The hydration time seems not to change the conductivity of the membrane pronouncedly. As shown in Figs. 11 and 12, ionic conductivity of membranes increases several orders of magnitude after 1 h immersion in water, and remains within the same order of magnitude for higher hydration time.

3.4.3. Potential application to an alkaline polymer electrolyte fuel cell

The ionic conductivity of the chitosan membrane may be useful for an alkaline polymer electrolyte fuel cell where a carrier type membrane for hydroxide ion transport is needed. Typical electrode reactions for the alkaline polymer electrolyte fuel cell are as follows [31]:

The net anode reaction:

$$2H_2 + 4OH^- \rightarrow 4H_2O + 4e^- \quad (5)$$

The net cathode reaction:

$$O_2 + 2H_2O + 4e^- \rightarrow 4OH^- \quad (6)$$

As shown in Eqs. (5) and (6), as long as the water and the hydroxide ions are supplied continuously, the chitosan membrane can act as a hydroxide ion carrier and the fuel cell can work in an uninterrupted way. In addition, the tensile strength of chitosan membranes is also high enough for this purpose. For a comparison, the Nafion® N117 membrane, which is the most effective and available membrane used in practical fuel cell systems [32], has a tensile strength in the dry state ca. 43 MPa [33]. Some chitosan membranes obtained in this work have a tensile strength of the same order. Although the ionic conductivity of chitosan membranes at present is about two orders of magnitude lower than Nafion® N117 which shows an ionic conductivity around 2.6×10^{-2} S cm^{-1} [34], the ionic conductivity of chitosan membranes can be improved significantly by modifying the hydroxyl groups or amino groups with suitable chemical or physical methods. However, a fundamental difference for the ionic functionality between the Nafion® N117 membrane and chitosan membranes has to be pointed out, that is, the Nafion® N117 membrane is a proton conductor and it only can be used for an acidic polymer electrolyte fuel cell, while the chitosan membrane is a hydroxide ion conductor and it may be used for an alkaline polymer electrolyte fuel cell. Further investigations for the ionic conductivity of chitosan membrane and their possible applications in alkaline polymer electrolyte fuel cell are being conducted in this group and relevant results will be reported in separate reports.

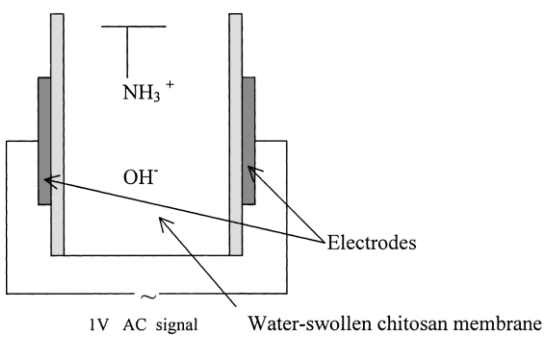

Fig. 13. Tentative mechanism of ionic conductance in swollen chitosan membrane.

4. Conclusion

Chitosan membranes with various DDA and MW were prepared. The crystalline structure of the membranes remained unchanged while their crystallinity degree increased with increasing DDA or with decreased MW of chitosan. The mechanical properties of membranes prepared from high DDA and high-molecular-weight chitosans were enhanced. The effects from the DDA and MW of chitosan on the SI of membrane showed a contrary tendency, that is, SI increased with the increase in MW of chitosan but decreased with increasing DDA. These chitosan membranes were not conductive in their dry state. In a suitable swollen state, an intrinsic ionic conductivity in the membrane as high as 10^{-4} S cm^{-1} could be reached. By using high MW and low DDA chitosan, the ionic conductivity of membranes is enhanced. A tentative mechanism for ionic conduction of chitosan membranes is suggested and a future application in alkaline polymer electrolyte fuel cells is predicted.

Acknowledgements

The financial support for this work was provided by the National Science and Engineering Council of Canada under the Strategic Grants Program (No. 239090-01).

References

[1] Shahidi F. Can Chem News 1995;47(8):25.
[2] Rathke T, Hudson S. J Macromol Sci, Rew Macromol Chem Phys 1994;C34:375.
[3] Kurita K, Inoue S, Nishimura S. J Polym Sci Part A: Polym Chem 1991;29:937.
[4] Kurita K, Inoue S, Koyam Y, Nishimura S. Macromolecules 1990;23: 2865.
[5] Muzzaralli RAA, Tanfani F, Emanuelli M, Mariotti S. Carbohydr Res 1982;107:199.
[6] Terbojevich M, Carraro C, Aosani A. Makromol Chem 1989;190: 2847.
[7] Moore GK, Roberts GAF. Int J Biol Macromol 1982;4:246.
[8] Muzzaralli RAA, Tanfani F. Carbohydr Polym 1985;5:297.
[9] Brine C, Sandford P, Zikakis J, editors. Advances in chitin and chitosan. New York: Elsevier; 1992.
[10] Arshady R, editor. Functional polymer, synthesis and application. Washington DC: American Chemical Society; 1996. p. 240.
[11] Phillip B, Dautzenberg H, Linow KJ, Kotz J. Prog Polym Sci 1989;14: 91.
[12] Uragami T, Yoshida F, Sugihara M. Makromol Chem Rapid Commun 1983;4:99.
[13] Roberts GAF. Chitin chemistry. London: Macmillian Press; 1992. p. 65.
[14] Maghami GG, Roberts GAF. Makromol Chem 1988;189:195.
[15] Muzzarelli RAA, Jeuniaux C, Gooday GW. Chitin in nature and technology. New York: Plenum; 1986. p. 385.
[16] Muzzarelli RAA, Rocchetti R. Carbohydr Polym 1985;5:461.
[17] Baxter A, Dillon M, Taylar KDA, Roberts GAF. Int J Biol Macromol 1992;14:166.
[18] Rabek JK. Experimental methods in polymer chemistry: applications of wide-angle X-ray diffraction (WAXD) to the study of the structure of polymers. Chichester, UK: Wiley-Inter Science; 1980. p. 505.
[19] Mokrini A, Acosta LJ. Polymer 2001;42:8817.
[20] Knaul JZ, Kasaai MR, Bui VT, Creber KAM. Can J Chem 1998;76: 1699.
[21] Kasaai MR, Arul JA, Charlet G. Proceedings of the seventh International Conference on Chitin and Chitosan. Lyon, France; 1998. p. 421.
[22] Salmon SI. The influence of physical form and annealing conditions on dye sorption by chitosan. PhD Thesis, North Carolina State University, Raleigh, NC, USA; 1995.
[23] Samuels RJJ. J Polym Sci, Polym Phys Ed 1981;19:1081.
[24] Anthonsen WM, Varum KM, Smidsrod O. Carbohydr Polym 1993;22: 193.
[25] Chen RH, Lin JH, Yang MH. Carbohydr Polym 1996;31:141.
[26] Blair HS, Guthrie J, Law TK, Tuekington P. J Appl Polym Sci 1987; 33:641.
[27] Maxfield J, Mandelkern L. Macromolecules 1977;10:1141.
[28] Kesting RE. Synthetic polymeric membranes. New York: McGraw-Hill; 1985.
[29] Beattie PD, Orfino FP, Basura VI, Zychowska K, Ding J, Chuy C, Schmeisser J, Holdcroft S. J Electroanal Chem 2001;503:45.
[30] Osman Z, Ibrahim ZA, Arof AK. Carbohydr Polym 2001;44:167.
[31] Barendrecht B. In: Blomen LJMJ, Mugerwa MN, editors. Fuel cell system. New York: Plenum Press; 1993. p. 88.
[32] Gottesfeld S, Zawodzinski TA. Electrochem Sci Eng 1997;5:195.
[33] Sondheimer SJ, Bunce NJ, Fyfe CA. J Macromol Sci, Rew Macromol Chem Phys 1986;C26:353.
[34] Sumner JJ, Creager SE, Ma JJ, DesMarteau DD. J Electrochem Soc 1998;145:107.